Figure S1. Related to Figure 1

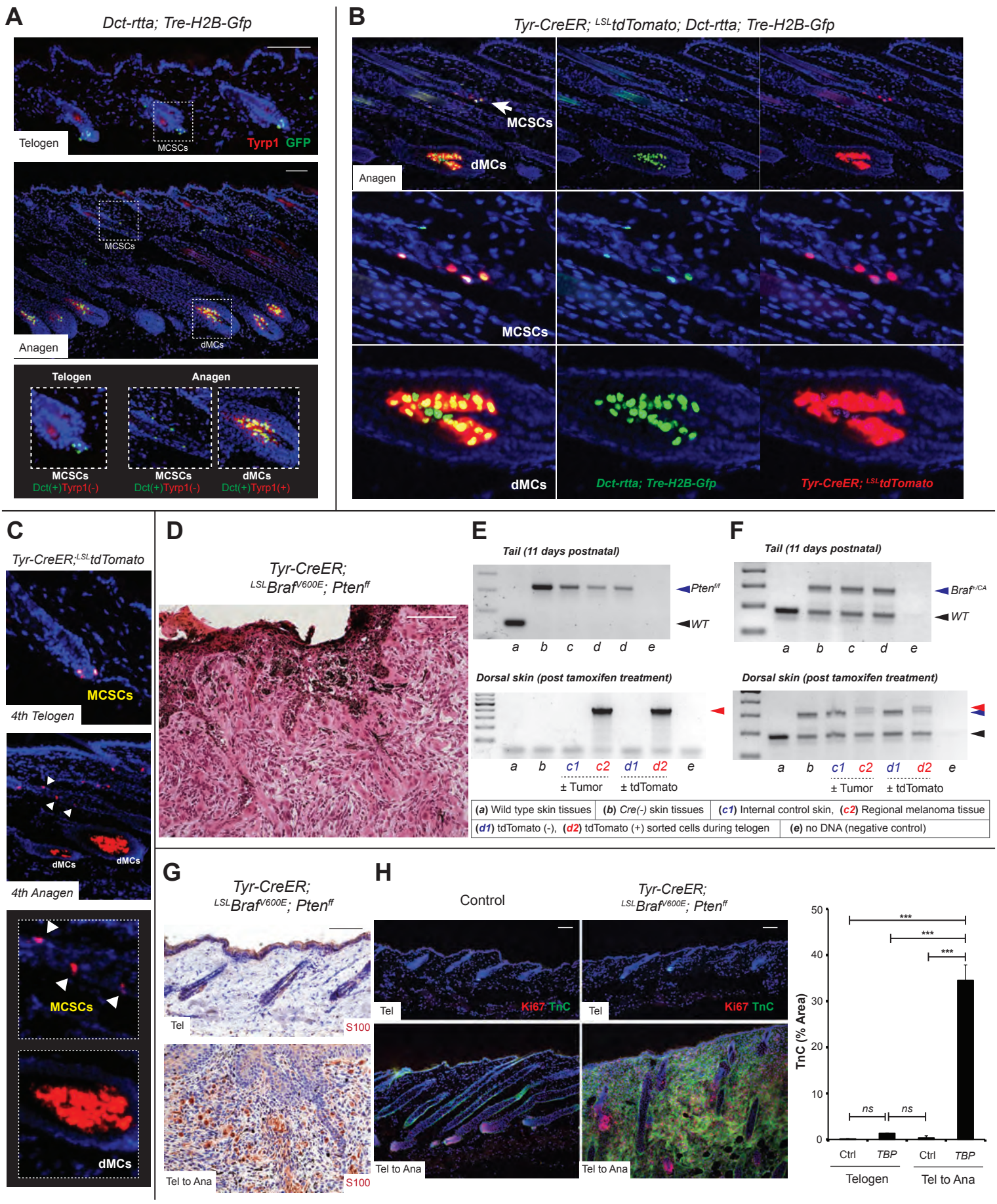

Figure S1 (Related to Figure 1). Co-labeling of tdTomato and H2B-GFP, histology and immunostaining for melanoma markers.

(A) Staining showing Dct^+ melanocyte stem cells (MCSCs) in telogen, with an absence of $Tyrp1^+$ melanocytes. Anagen follicles demonstrate $Dct^+/Tyrp1^+$ (double positive) melanocytes in the hair bulb. (B) Co-expression of tdTomato and H2B-GFP in MCSCs and melanocytes of the hair bulb was examined in *Tyr-CreER; LSL-tdTomato; Dct-rtta; Tre-H2B-Gfp* mice. Mice were treated with drinking water containing doxycycline and intraperitoneal injection of tamoxifen to visualize MCSCs at the bulge region and differentiated melanocytes (dMCs) in the hair bulb during anagen. (C) Tamoxifen was injected when mice were 8 weeks postnatal and in the telogen state. After four hair cycles, skin was collected and tdTomato expression from MCSCs were observed in the hair germ, and in the differentiated progeny of the hair bulb. (D) Histology was performed for late stage melanocytic tumor tissues originated from tumor-prone melanocyte stem cells. (E-F) PCR analysis shows the presence of wild type (black arrow heads) or mutant genetic alleles (blue arrow heads) as well as Cre-mediated genetic recombination (red arrow heads): a, control mice; b, *LSL-$Braf^{V600E}$; $Pten^{lf}$* mice; c and d, *Tyr-CreER; LSL-$Braf^{V600E}$; $Pten^{lf}$; LSL-tdTomato* mice. Internal control skin (c1) was not exposed to tamoxifen. (G) Immunohistochemistry for the melanoma marker S100 was performed for the skin from *Tyr-CreER; LSL-$Braf^{V600E}$; $Pten^{flox/flox}$* (TBP) mice (H) Immunostaining for the melanoma marker Tenascin-C (TnC) and a proliferation marker Ki67 was performed in control and TBP mice. Data are represented as mean ± SEM. $n \geq 40$ fields from 8 control mice, and $n \geq 60$ fields, 8 TBP mice. Tel, telogen; Ana, anagen. Scale bar, 100 μm.

Figure S2. Related to Figure 1

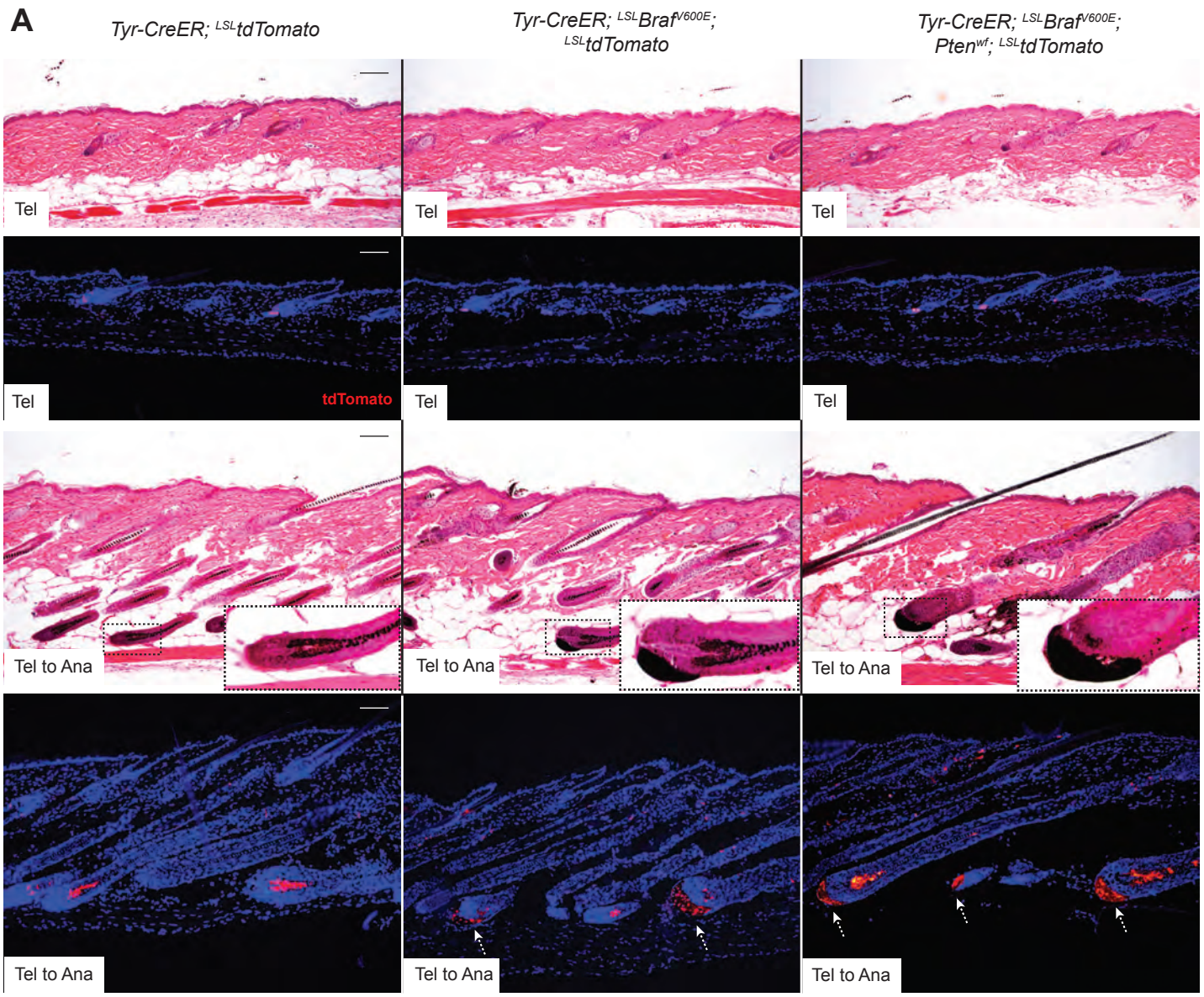

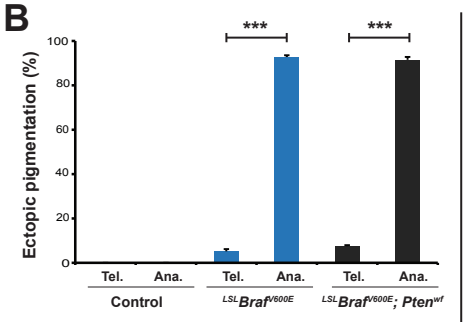

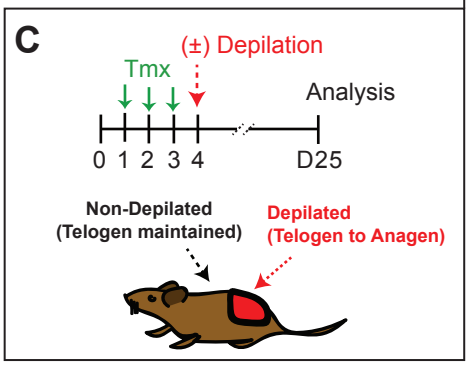

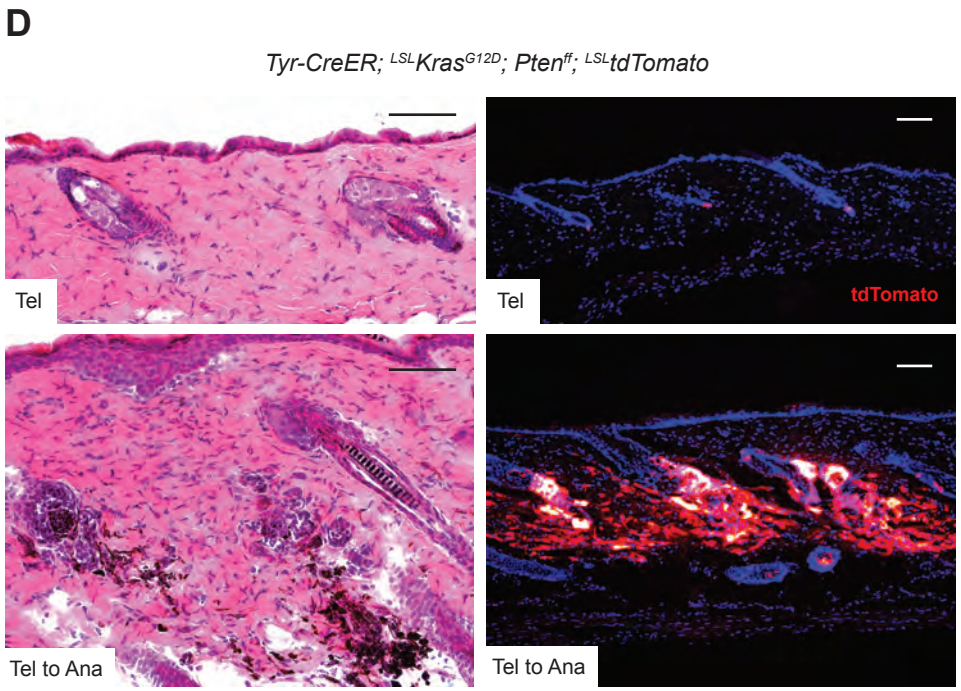

Figure S2 (Related to Figure 1). *Braf*^{V600E}-driven nevogenesis and *Kras*^{G12D}-driven melanomagenesis requires melanocyte stem cell activation.

(A) Histology and tdTomato lineage tracing showed ectopic pigmentation in *Tyr-CreER; LSL-Braf*^{V600E}*; LSL-tdTomato* (TBT) and *Tyr-CreER; LSL-Braf*^{V600E}*; Pten*$^{wt/flox}$*; LSL-tdTomato* (TBP^{wf}T) mice. (B) Ectopic pigmentation was quantified using at least 200 hair follicles per condition/mouse. Data are represented as mean ± SEM. n = 7 TBT and n = 6 TBP^{wf}T mice. (C) Experimental scheme. Tmx, tamoxifen. (D) Melanoma development is observed by histology and tdTomato lineage tracing following melanocyte stem cell activation (anagen) in *Tyr-CreER; LSL-Kras*^{G12D}*; Pten*$^{flox/flox}$*; LSL-tdTomato* mice. Tel, telogen; Ana, anagen. Scale bar, 100 µm.

Figure S3. Related to Figure 2

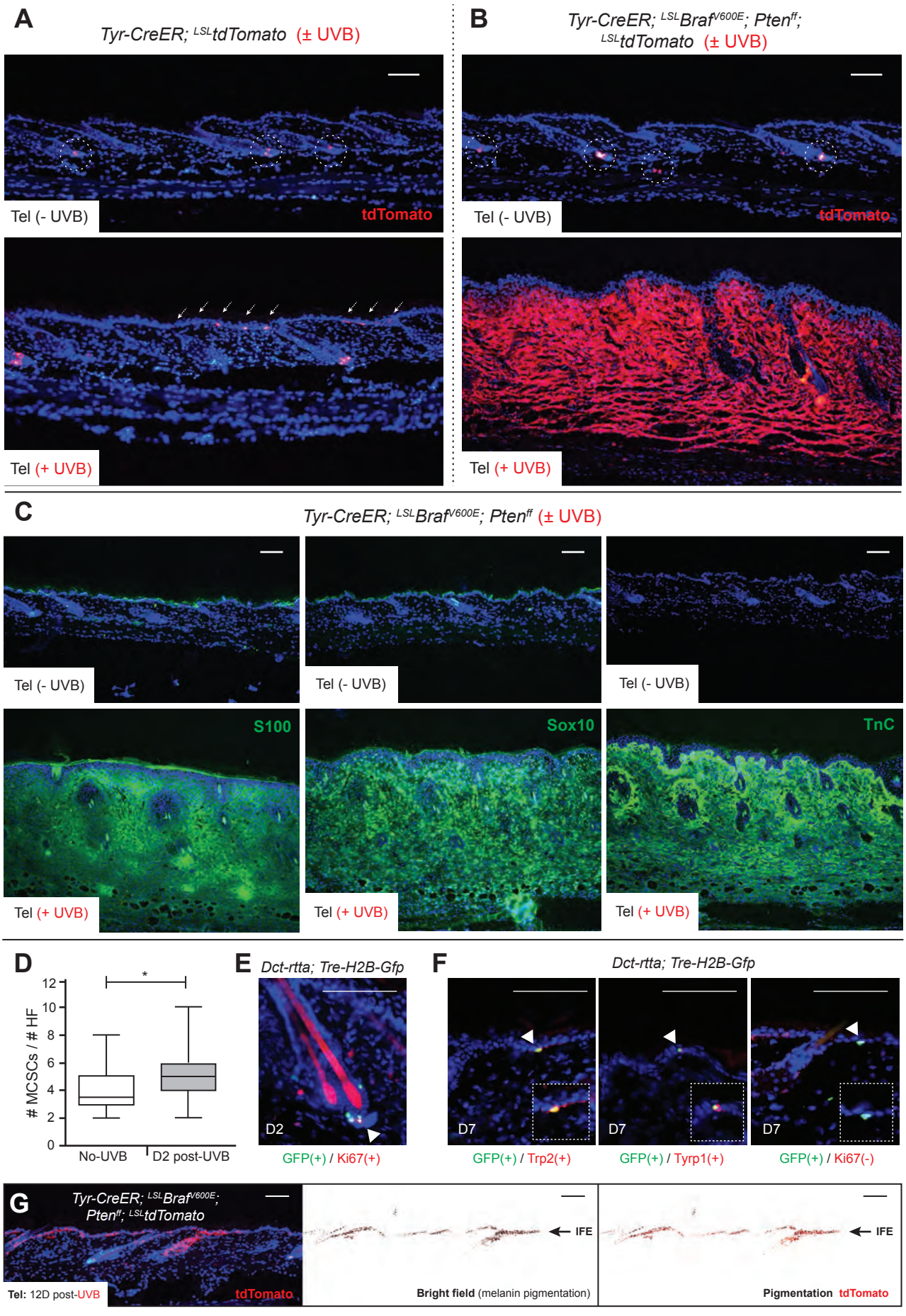

Figure S3 (Related to Figure 2). Ultraviolet radiation initiates melanoma development from quiescent tumor-competent melanocyte stem cells (MCSCs).

(A) tdTomato lineage tracing reveals UVB-mediated melanocyte stem cells (MCSC) translocation (white arrows). (B) UVB-induced melanomagenesis was observed using tdTomato lineage tracing in *Tyr-CreER; LSL-Braf^{V600E}; Pten$^{flox/flox}$; LSL-tdTomato* mice. However, quiescent tumor-competent MCSCs (white circles) were unable to develop melanomas. (C) Immunostaining for melanoma markers, S100, Sox10, and TnC was performed in non-UVB and UVB-exposed skin of *Tyr-CreER; LSL-Braf^{V600E}; Pten$^{flox/flox}$* (TBP) mice. (D-E) Relative number of MCSCs was determined through GFP lineage tracing in *Dct-rtta; Tre-H2B-Gfp* mice. Representative figure of Ki67 positive MCSCs 2 days after UVB irradiation. (F) Post-migrated TRP2^{+} (Dct^{+}) melanocytes express a differentiated melanocyte marker (Tyrp1^{+}) but not a proliferative marker (Ki67^{-}) in *Dct-rtta; Tre-H2B-Gfp* mice. (G) Post-UVB exposure, migrating/migrated melanocytes originated from melanoma-prone MCSCs in TBP mice represent continued proliferation and differentiation showing both tdTomato and melanin pigment. Tel, telogen. Scale bar, 100 μm.

Figure S4. Related to Figure 2

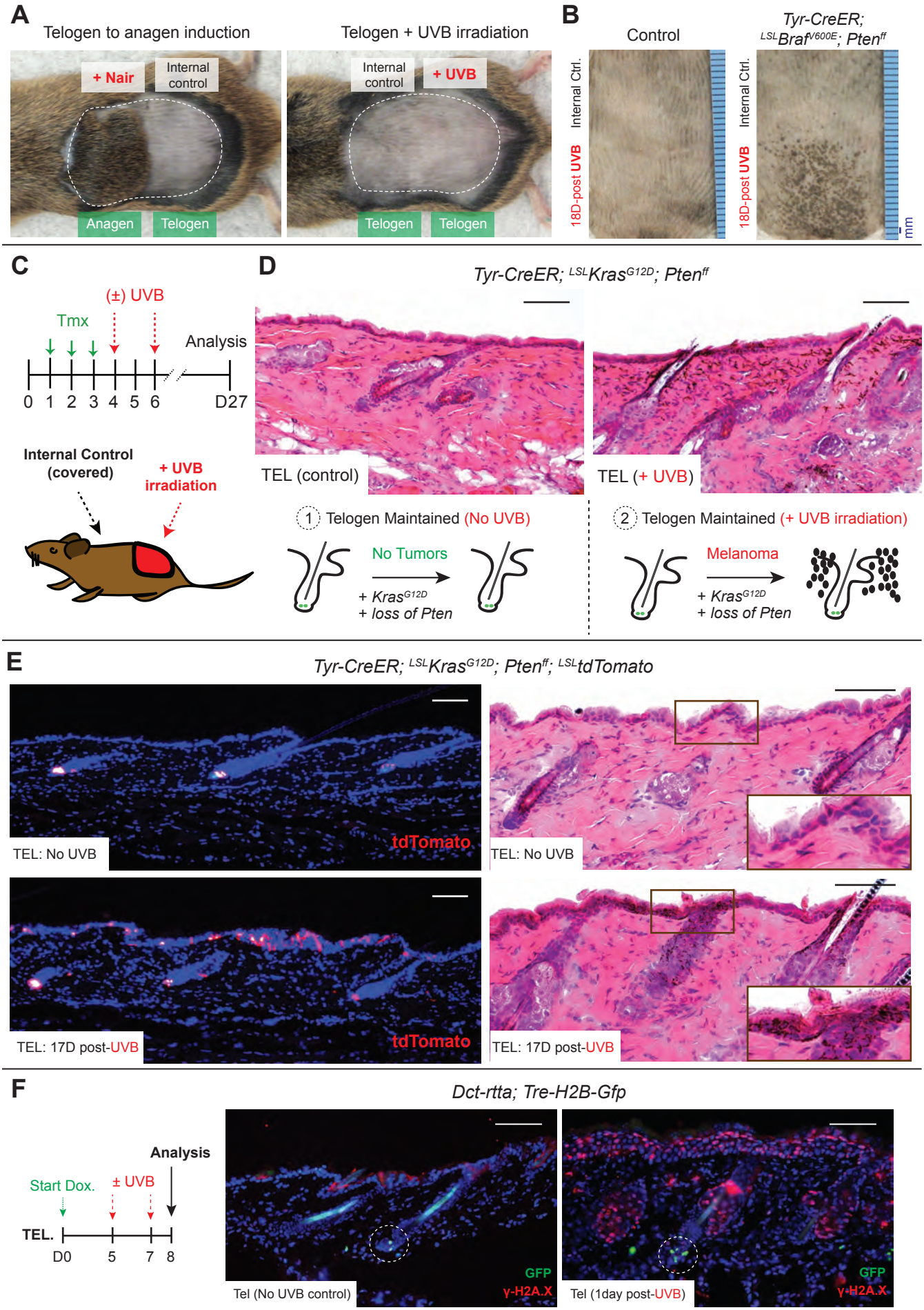

Figure S4 (Related to Figure 2). Ultraviolet-B radiation exposure stimulates *Kras^{G12D}*-driven melanoma initiation in quiescent melanoma-competent MCSCs.

(A-B) When mice were 7 weeks postnatal, artificial anagen induction was performed by chemical depilation (+ Nair). Unlike Nair treatment, UVB irradiation did not show anagen induction (+ UVB). Despite lack of anagen induction, UVB irradiation was sufficient to induce melanocytic hyperplasia in the skin of *Tyr-CreER; LSL-Braf^{V600E}; Pten$^{flox/flox}$* mice (18 days post-UVB). (C-D) Experimental scheme, histology and summary of *Kras^{G12D}*-driven melanoma initiation. After intraperitoneal tamoxifen (Tmx) injections, UVB was irradiated onto the skin of *Tyr-CreER; LSL-Kras^{G12D}; Pten$^{flox/flox}$* mice. Histology demonstrates no tumor initiation in non-UVB skin but melanoma development in the skin by UVB exposure. (E) Lineage tracing and histology demonstrate *Kras^{G12D}*-driven early melanomagenesis at the IFE by UVB exposure. (F) Drinking water containing doxycycline (Dox) was administered 5 days prior to UVB treatment, and skin tissues were collected after UVB irradiation in *Dct-rtta; Tre-H2B-Gfp* mice. A marker of DNA damage response, γ-H2A.X (red), was positive in numerous cells of epidermis but not in MCSCs at the hair germ (green). Tel, telogen. Scale bar, 100 μm.

Figure S5. Related to Figure 6

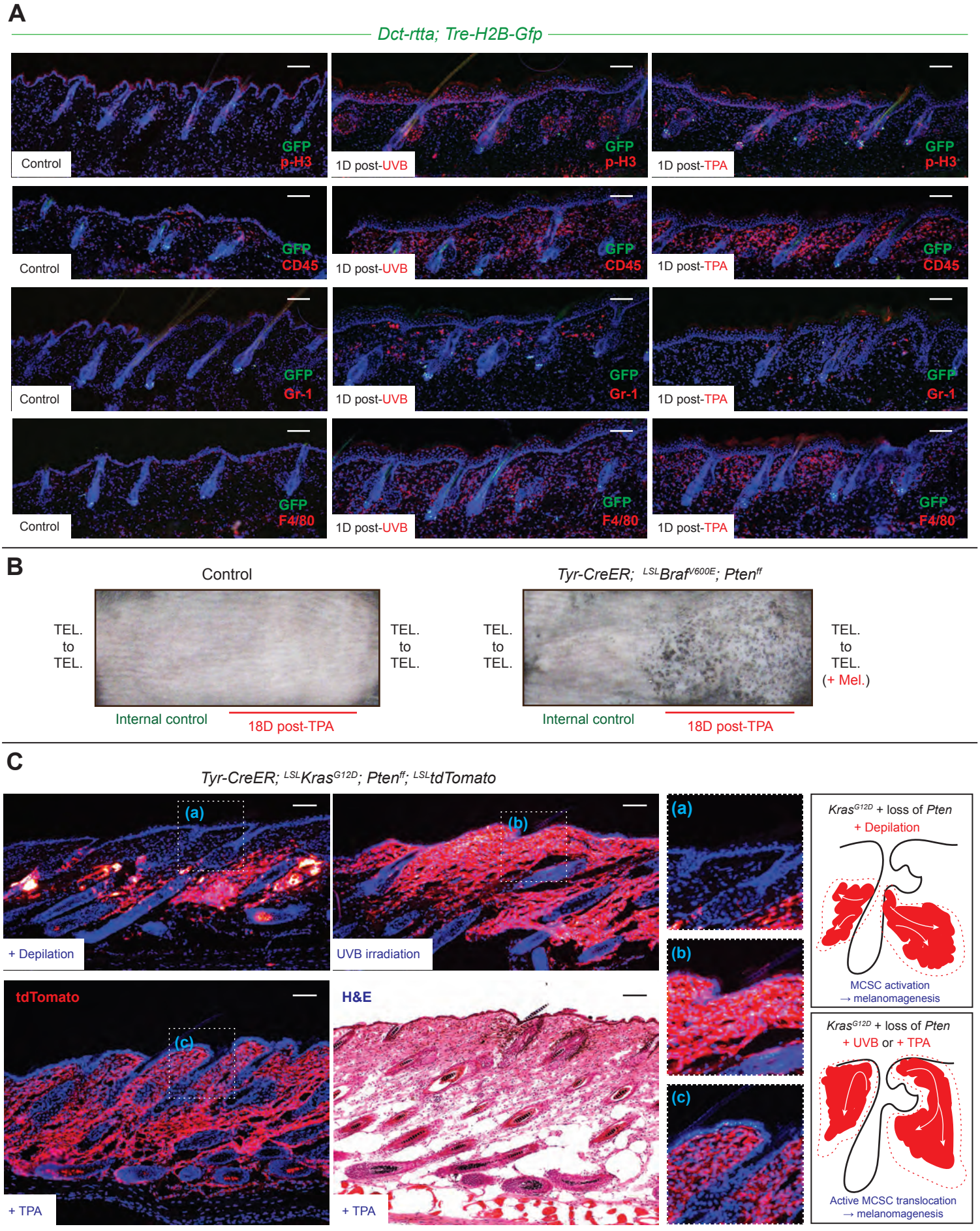

Figure S5 (Related to Figure 6). UVB-irradiation and TPA-treatment initiate melanoma associated the epidermis.

(A) Immunostaining was performed for a proliferative marker (phospho-Histone H3), and CD45, Gr-1 and F4/80 immune cell recruitment in UVB-irradiated or TPA-treated skin tissues in *Dct-rtta; Tre-H2B-Gfp* mice. Scale bar, 100 μm. (B) Similar to UVB, while short-term TPA treatment was not sufficient to induce anagen (control dorsal skin), macroscopically induced melanocytic hyperplasia was significantly observed in the dorsal skin of *Tyr-CreER; LSL-Braf*^{V600E}*; Pten*$^{flox/flox}$ mice. TEL., telogen; MEL., melanocytic hyperplasia. (C) Lineage tracing tdTomato shows differentially regulated *Kras*^{G12D}-driven melanomagenesis by UVB and TPA compared to anagen induction by chemical depilation. Tel, telogen. Scale bar, 100 μm.

Figure S6. Related to Figure 6

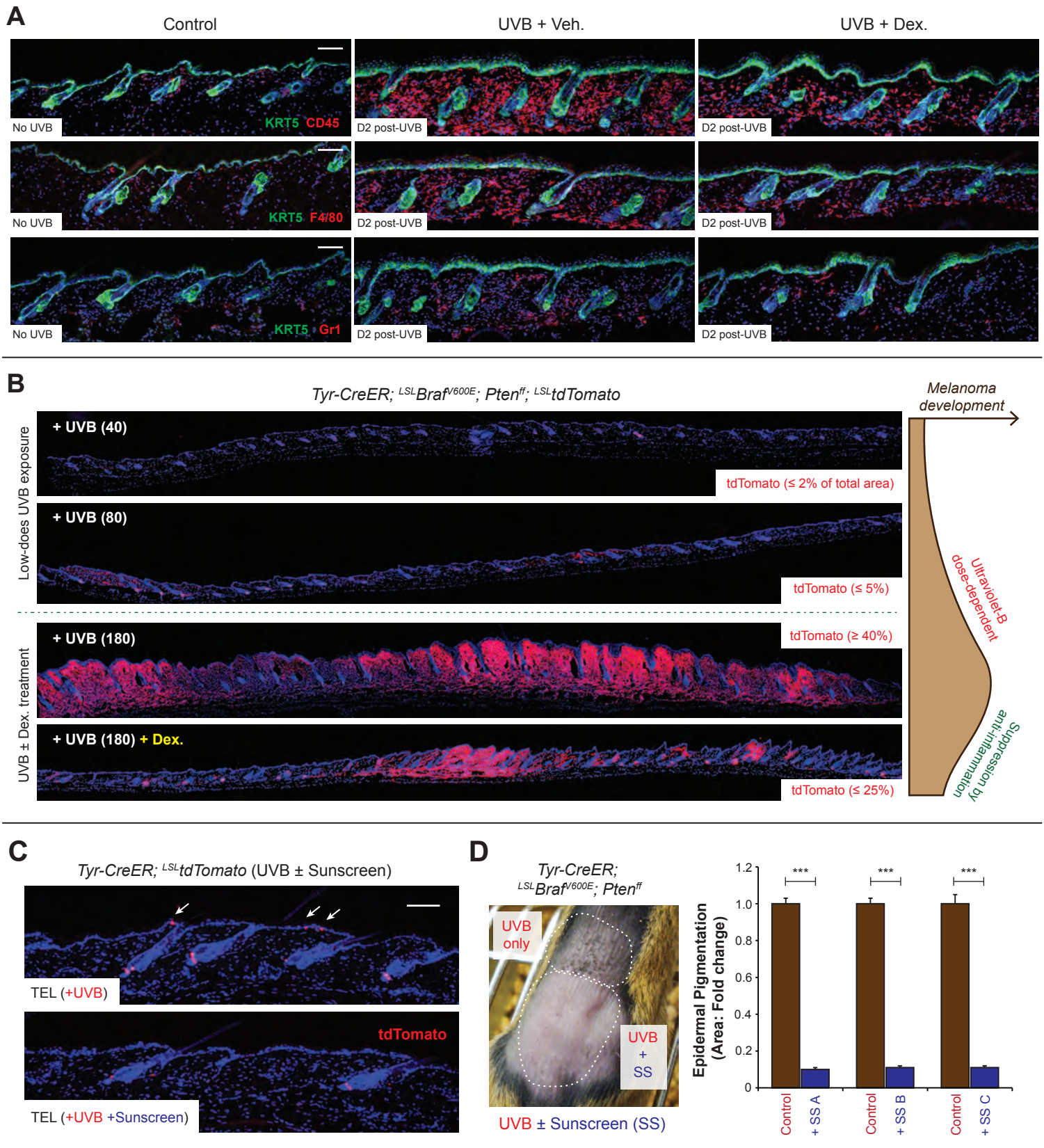

Figure S6 (Related to Figure 6). Dexamethasone treatment and sunscreen application can attenuate cutaneous melanomagenesis upon UVB exposure. (A) Immunostaining for CD45, F4/80 and Gr-1 immune cell recruitment shows attenuation of UVB-induced acute inflammation by dexamethasone treatment. Veh., vehicle treatment. Dex., dexamethasone treatment. Scale bar, 100 μm. (B) Lineage tracing tdTomato represents the burden of melanoma development in low-dose UVB exposure or UVB radiation with/without dexamethasone treatment. The reconstructed panoramic images for tdTomato lineage tracing were shown by reconstructed sequential photomicrographs. Low-dose 40, 40 mJ cm^{-2} UVB; low-dose 80, 80 mJ cm^{-2} UVB; UVB, 180 mJ cm^{-2}; Dex., dexamethasone treatment. (C) Suppressed UVB-mediated MCSC translocation by sunscreen application was observed through tdTomato lineage tracing. (D) Macroscopic changes in UVB-mediated melanomagenesis with application of 3 different commercially available sunscreens, and quantification of epidermal pigmentation by melanoma development. Data are represented as mean ± SEM. $n = 6$ per each group. Counter staining, DAPI. Scale bars, 100 μm.

Figure S7. Related to Figure 7

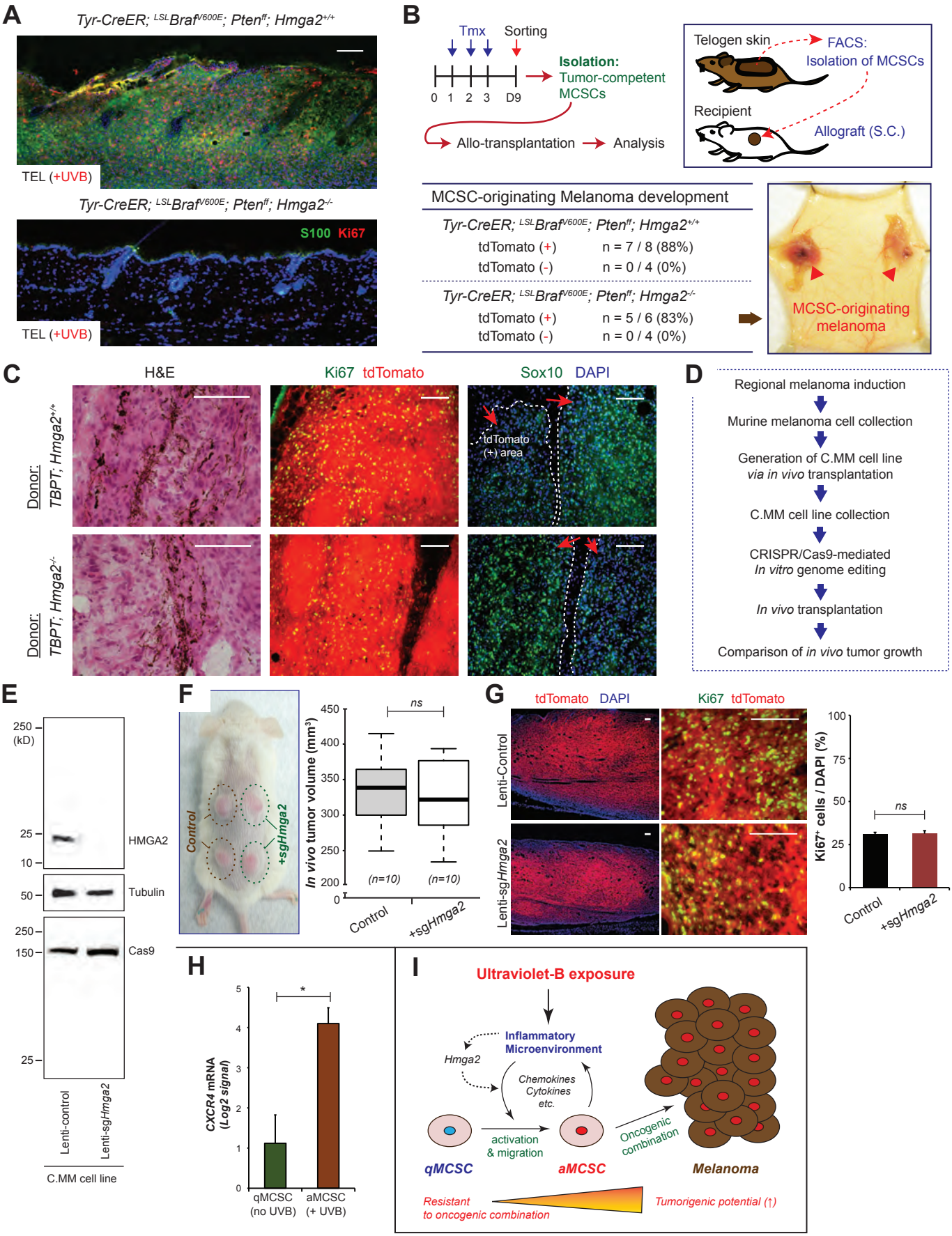

Figure S7 (Related to Figure 7). Intrinsic expression level of *Hmga2* does not significantly affect tumor-prone MCSC-originating melanoma development and *in vivo* melanoma growth rate.

(A) Immunostaining for the melanoma marker S100 and a proliferation marker Ki67 was performed in *Tyr-CreER; LSL-Braf^{V600E}; Pten$^{flox/flox}$; Hmga2$^{+/+}$* (TBP; *Hmga2$^{+/+}$*) and *Tyr-CreER; LSL-Braf^{V600E}; Pten$^{flox/flox}$; Hmga2$^{-/-}$* (TBP; *Hmga2$^{-/-}$*) mice. Tel, telogen. Scale bar, 100 μm. (B) Experimental scheme and the frequency of melanoma development from tumor-prone melanocytes stem cells (MCSCs) sorted from TBP; *Hmga2$^{+/+}$* and TBP; *Hmga2$^{-/-}$* mice, as well as the resulting tumors. The contingency table shows no statistical significance in Fisher's exact test. (C) Representative figures show histology and immunostaining for lineage tracing tdTomato, proliferation marker Ki67 and melanoma marker Sox10. (D) Experimental scheme. Cornell Murine Melanoma (C.MM) cell line was established *via* transplantation using murine melanoma cells from TBPT mice. (E) Western blotting was performed for control and *Hmga2* gene-edited C.MM cell lines. Loading control, α-tubulin. (F) Macroscopic phenotypes of transplanted control and experimental C.MM cells and final tumor volume determined by a modified ellipsoid formula. Mean ± SEM. *n* = 10. *ns* = not significant. (G) Immunostaining shows a lineage tracing marker, tdTomato, and a proliferation marker, Ki67. Relative number of Ki67 positive cells were counted at the high-power fields. Mean ± SEM. *n* = 10. *ns* = not significant. Counter staining, DAPI. Scale bars, 100 μm. (H) Relative mRNA expression of *Cxcr4* was measured by RNAseq using sorted quiescent tumor-prone MCSCs (qMCSC, no UVB) and UVB-induced early melanoma cells (aMCSC, +UVB). Mean ± SEM, *n* = 3. (I) Summary of the role of extrinsic stimulus UVB in

melanoma initiation from quiescent melanoma-competent MCSCs *via* inflammatory-mechanisms and microenvironmental *Hmga2* expression dependent processes.

Table S1. (Related to STAR method) Oligonucleotide sequences.

Gene of Interest	Name	Sequence	Source
KrasG12D	K005	AGCTAGCCACCATGGCTTGAGTAAGTCTGCA	NCI Mouse Repository
	K006	CCTTTACAAGCGCACGCAGACTGTAGA	
Cre	Cre3	GCATTACCGGTCGATGCAACGAGTGATGAG	Jackson Laboritories
	Cre5	GAGTGAACGAACCTGGTCGAAATCAGTGCG	
Pten	IMR 9554	CAAGCACTCTGCGAACTGAG	Jackson Laboritories
	IMR 9555	AAGTTTTTGAAGGCAAGATGC	
	Pten-1	ACTCAAGGCAGGGATGAGC	Lesche et al., 2002
	Pten-2	AATCTAGGGCCTCTTGTGCC	
	Pten-3	GCTTGATATCGAATTCCTGCAGC	
Braf	Braf-F	TGAGTATTTTTGTGGCAACTGC	Jackson Laboritories
	Braf-R	CTCTGCTGGGAAAGCGGC	
Tomato	TWTF	AAGGGAGCTGCAGTGGAGTA	Jackson Laboritories
	TWTR	CCGAAAATCTGTGGGAAGTC	
	TMR	GGCATTAAAGCAGCGTATCC	
	TMF	CTGTTCCTGTACGGCATGG	
Dct-rtta	Y-104	ACTAAGTAAGGATCAATTCAG	NCI Mouse Repository
	Y-105	TGTACTAGGCAGACTGTG	
Tre-H2B Gfp	Y-106	GCCACAAGTTCAGCGTGTCC	NCI Mouse Repository
	Y-107	GATGCCCTTCAGCTCGATGC	
Hmga2	H. Wild Type	GTGTCCCTTGAAATGTTAGGCGGGG	Anand & Chada, 2000
	H. Common	CCCACTGCTCTGTTCCTTGC	
	H. Null	AGGAGCCAAGCTGCTATTGG	
	Hmga2-F	AAGGCAGCAAAAACAAGAGC	Boumahdi et al., 2014
	Hmga2-R	CCGTTTTTCTCCAATGGTCT	
β-actin	Actb-F	GATTACTGCTCTGGCTCCTAGC	
	Actb-R	GACTCATCGTACTCCTGCTTGC	